Ion-beam-induced modification of fullerene films as studied by electron-energy-loss spectroscopy

A. Hoffman
Chemistry Department and Solid State Institute, Technion, Haifa 32000, Israel

P. J. K. Paterson and S. T. Johnston
Department of Applied Physics, Royal Melbourne Institute of Technology, 124 Latrobe Street, Melbourne 3001, Australia

S. Prawer
School of Physics, University of Melbourne, Parkville, Victoria 3052, Australia
(Received 22 March 1995)

The ion-beam (2 keV Ar) -induced amorphization of thin fullerene films has been studied by *in situ* electron-energy-loss spectroscopy (EELS). With due care to the electron-beam current, the EELS spectrum may be measured without degradation during the electron bombardment to provide an EELS fingerprint of C_{60} films. The diminution of the intensity of characteristic peaks in the EELS spectrum upon ion impact was used to deduce a cross section for the destruction of the C_{60} molecules of $(0.85\pm0.2)\times10^{-14}$ cm^2. This value corresponds closely to the geometric size of one C_{60} molecule, suggesting that each incident Ar ion destroys one C_{60} molecule upon ion impact. This cross section is somewhat smaller than that expected using scaling arguments from the results of more energetic ion bombardment (100–300 keV). The difference may be due to surface processes, which become important for low-energy ion-beam irradiation.

INTRODUCTION

The interaction of fullerene films with energetic laser and ion beams is a topic of considerable current interest. Both fragmentation[1] and polymerization[2] of the molecule can be observed under the appropriate conditions. The mechanism of fragmentation gives important clues as to the structure and bonding of the molecule.[3]

In previous work, we have studied the fragmentation of C_{60}, using energetic (640 keV) heavy-ion (Xe) beams.[4,5] As a result of a careful study of the dose dependence of the conductivity of fullerene films subjected to ion irradiation,[4] it was concluded that upon ion impact each molecule explodes into its constituent C atoms. Support for this proposition also came from a Raman and infrared study of fullerene films irradiated with 640-keV Xe ions.[5] The latter study also concluded that the mechanism for the destruction was nuclear knock-on collisions, rather than by some electronic process. A similar conclusion has recently been published by Kastner, Kuzmany, and Palmetshofer.[6] The Raman studies[5] allowed the extraction of a cross section, σ, for the destruction of C_{60} of 6×10^{-13} cm^2. This large cross section gives an equivalent effective radius of about 4.2 nm, which is much bigger than the geometric radius of the C_{60} molecule (0.35 nm). This large radius may be attributed to the effect of secondary knock-on processes. The passage of each Xe ion through the fullerene film gives rise to a collision cascade, in which the C atoms knocked on by the Xe ion themselves damage and destroy other C_{60} molecules.

In the present work, we investigate the response of C_{60} to 2-keV Ar-ion irradiation, using electron-energy-loss spectroscopy (EELS) as our main analysis tool. We investigate whether the cross section for destruction scales with nuclear energy loss if low-energy (2 keV) ions are used. The use of a surface sensitive technique such as EELS means that we were primarily sensitive to the surface layer of fullerene molecules, rather than the bulk. Extraneous effects, such as contamination by air, were completely eliminated as the films were irradiated and analyzed *in situ* in a UHV environment. The results suggest that each C_{60} does indeed disintegrate when struck by an incident Ar ion; however, the cross section is much lower than that expected on the basis of the comparison of the results for C_{60} films bombarded with ions with kinetic energies of the order of 100 keV.

EXPERIMENT

The C_{60} films, approximately 200 nm thick, were deposited on silicon substrates by thermal evaporation of a purified C_{60} powder at room temperature. Raman spectra of the films revealed all the expected peaks due to C_{60},[7,8] with no evidence of peaks due to amorphous carbon or other fullerenes. For comparison to well ordered graphite, samples of freshly cleaved highly oriented pyrolytic graphite (HOPG) were also analyzed.

The as-deposited films were placed in a MLAB 310-F Auger nanoprobe equipped with a hemispherical analyzer, field-emission electron gun, and a secondary electron detector. The base vacuum was 2×10^{-10} Torr. Examination of the surface of the films using the scanning electron microscope mode of the nanoprobe revealed the films to be smooth and pin-hole free. High sensitivity Auger measurements revealed C as the only constituent of the films.

The films were analyzed by EELS over the loss range 0–40 eV. A primary energy of 1.0 keV was used with a full width at half maximum of 0.8 eV, and a primary current of 10^{-9} A. The electron-beam diameter was about 10 nm. The electron beam was incident at an angle of 30° to the sample normal, with an angle of 60° between the electron-beam direction and the entrance to the electron analyzer.

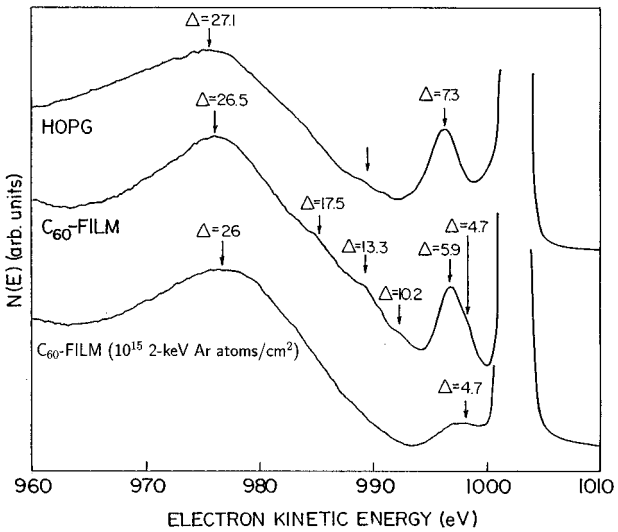

FIG. 1. The electron-energy-loss spectrum of highly oriented pyrolytic graphite, a pristine C_{60} thin film, and a C_{60} film, which has been irradiated with 1×10^{15} Ar/cm^2 at 2 keV.

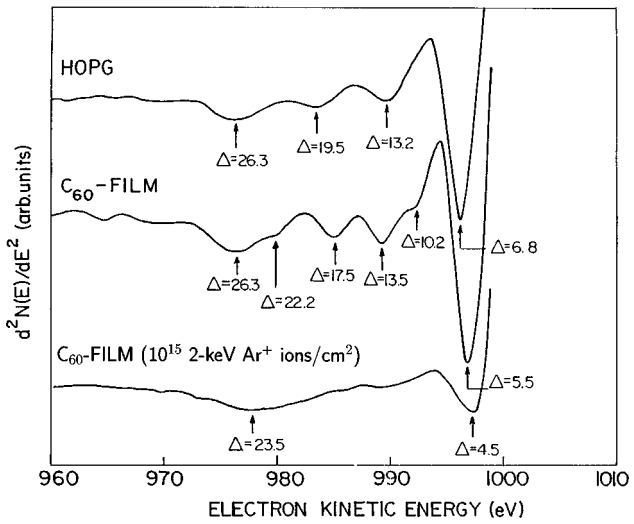

FIG. 2. The data of Fig. 1 displayed in the second derivative mode to enhance the visibility of the smaller peaks in the EELS spectrum.

In order to minimize beam damage to the sample, the electron-beam was scanned over an area of 1×1 mm^2. The EELS spectrum was recorded in reflection in the $N(E)$ vs E mode using a constant retardation ratio of 40, with steps of 0.2 eV. The detector resolution was better than 50 meV; hence, the spectral resolution was limited by the chromacity of the incident electron beam ($ie\pm0.8$ eV). A typical measurement took 150 s. Under these measurement conditions, even extremely long exposures to the electron beam (exceeding 5 h) did not lead to any degradation of the EELS spectrum or of the Raman spectrum.

The Ar-ion irradiation at 2 keV were performed using a differentially pumped ion gun at an angle of 50°, with respect to the sample normal. The ion flux was 1×10^{11} ions/cm^2/s. The ion beam was scanned over an area of 1×1 cm^2. The EELS spectrum was taken from an area in the center of the ion-irradiated region, thus avoiding edge effects.

RESULTS

Figure 1 shows the EELS spectrum of HOPG, pristine C_{60} and C_{60} irradiated to a dose of 1×10^{15} Ar/cm^2 displayed in the $N(E)$ vs E mode. The spectra have been normalized to the intensity of the zero loss peak. The main features of the HOPG spectrum are the π plasmon at 7.3 eV and the broad $\sigma+\pi$ plasmon centered at 27.1 eV. C_{60} shows similar broad features at energies of 5.9 and 26.5 eV. Figure 1(c) shows the spectrum of C_{60}, irradiated with 1×10^{15} Ar/cm^2. The result of the irradiation is that the π peak broadens and moves downward in energy. The spectrum shown in Fig. 1(c) is typical of that obtained for other carbons (such as HOPG and glassy carbon) irradiated to similar doses. Figure 1(c) is also similar to that obtained for as-deposited electron-beam evaporated amorphous carbon (a-C), except that the $\sigma+\pi$ peak is located at 26 eV for irradiated carbons and at 23 eV for a-C. The difference in peak position is attributable to the ion-beam-induced compaction of carbon, which leads to an upward shift in the $\sigma+\pi$ plasmon energy.[9]

In addition to the broad features mentioned above, the spectrum for HOPG and C_{60} display a number of shoulders, which become more obvious when the EELS spectrum is displayed in the second derivative mode as $d^2N(E)/dE^2$ vs E (see Fig. 2). For C_{60}, peaks at 10.2, 13.5, and 17.5 eV are evident. The peak at 10.2 eV has been ascribed to a single-electron transition. The 17.5-eV peak is probably attributable to the surface plasmon corresponding to the bulk plasmon at 26.5 eV. The 13.5-eV peak has been attributed[8,9] to a surface plasmon connected with the spherical shape of the C_{60} molecule. However, this peak is also present in the spectrum of HOPG; hence, this assignment is doubtful. This peak may, in fact, also be due to single-electron transitions. Despite the uncertainty in the peak assignments, the EELS spectrum can be used as a signature for the presence of C_{60}.

In Fig. 3, the EELS spectrum of C_{60} in the second derivative mode is displayed as a function of Ar-ion dose. The π peak at 5.9 eV decreases in intensity, broadens, and moves down in energy to the value typical for amorphous carbon (4.9 eV). The peaks at 13.5 and 17.5 eV gradually decrease in intensity, but do not shift in peak position. The 13.5-eV peak also does not broaden, while the 17.5-eV peak does display some peak broadening.

Figure 4 shows the energy of the π peak, as a function of ion dose. The intensities of the 13.5- and 17.5-eV peaks, as a function of ion dose, are shown in Fig. 5. Little change in these parameters is observed until a dose of about 1×10^{13} Ar/cm^2, with the ion-beam-induced changes saturating at a dose of about 1×10^{15} Ar/cm^2. As noted above, at this dose, the spectrum is very similar to that obtained from evaporated amorphous carbon; hence, it appears that at this dose the C_{60} layer has been completely amorphized, with no intact C_{60} clusters remaining in the affected volume.

DISCUSSION

Previous work[4–6] on the response of C_{60} thin films to ion irradiation in the keV energy range has concluded that (1) the

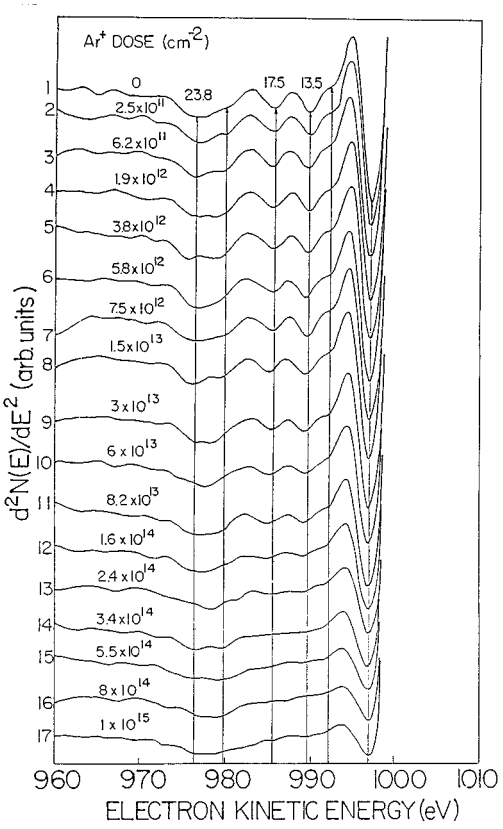

FIG. 3. The EELS spectrum of C_{60} irradiated with 2-keV Ar ions to doses up 1×10^{15} Ar/cm^2. The spectrum is displayed in the second derivative mode. Note the diminution of the intensity of the peaks at 13.5 and 17.5 eV, and the shift of the position of the π plasmon to lower energies.

dominant driving force for the ion-beam modification is atomic knock-on collisions (i.e., the energy deposited by the incident ion in nuclear collisions) and (2) each C_{60} molecule disintegrates upon ion impact into individual C (or possibly C_2 clusters). No large fullerene fragments are observable as a result of the irradiation.

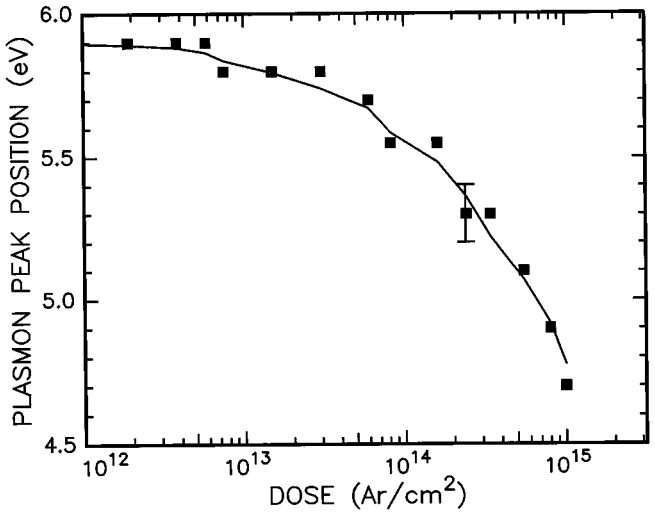

FIG. 4. The energy of the π plasmon peak, as a function of Ar- (2-keV) ion dose.

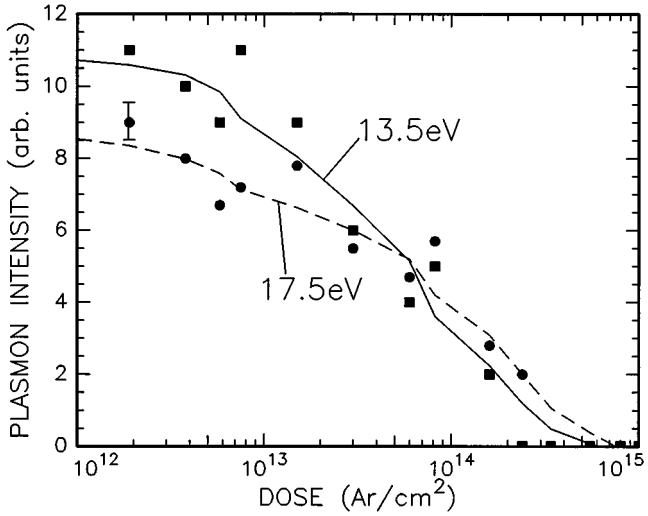

FIG. 5. The intensities of the 13.5- (squares) and 17.5- (circles) eV peaks, as a function of Ar- (2-keV) ion dose. The solid lines are a guide to the eye.

These conclusions were based on electrical conductivity measurements of the irradiated films[4] and *ex situ* Raman and IR measurements.[5] From the dose dependence of the diminution of the intensity of the dominant Raman peaks, it was possible to obtain an effective cross section, σ, for the destruction of C_{60} by ion impact of $(6\pm1.5)\times10^{-13}$ cm^2. The effective radius, $r_{\rm eff}$ of the fullerene for destruction by the ion beam is then given by $\pi(r_{\rm eff})^2=\sigma$, or $r_{\rm eff}=4.6$ nm, which is much larger than the geometric radius of a single C_{60} molecule. The large effective radius was explained in terms of the contribution of secondary processes to the destruction of C_{60} molecules. Each Xe ion can knock on many C atoms and these in turn can destroy other C_{60} molecules. Hence, the measured cross section in the previous work is much larger than might be expected on the basis of a geometric argument alone.

The present results also allow the extraction of an effective cross section for the destruction of C_{60}, but in this case by low-energy 2-keV Ar ions. The diminution of the intensities of the 13.5- and 17.5-eV peaks can be used to extract this cross section. We assume that the intensity of these peaks is proportional to the number of intact C_{60} clusters. Support for this proposition comes from the observation that these peaks do not shift in energy as a function of ion dose. Following the analysis suggested in Ref. 10, we assume that the areal density of intact C_{60} clusters, N, which remain after irradiation with an ion dose, D, is given by

$$N=N_0\,\exp(-\sigma D), \tag{1}$$

where σ is the effective cross section.

Hence, a plot of $\log_{10}(I(D)/I_0)$ versus D, where $I(D)$ is the intensity of either the 13.5- or 17.5-eV peaks after a dose D, and I_0 is the intensity of the respective peak in the pristine film, should yield a straight line whose slope is the effective cross section, σ, for destruction of C_{60} by the ion beam. In Fig. 6, the data of Fig. 4 for the intensity of the 13.5-eV peak has been plotted as $\log_{10}(I(D)/I_0)$ vs D, and a similar plot for the 17.5-eV peak is shown in Fig. 7. Indeed these plots

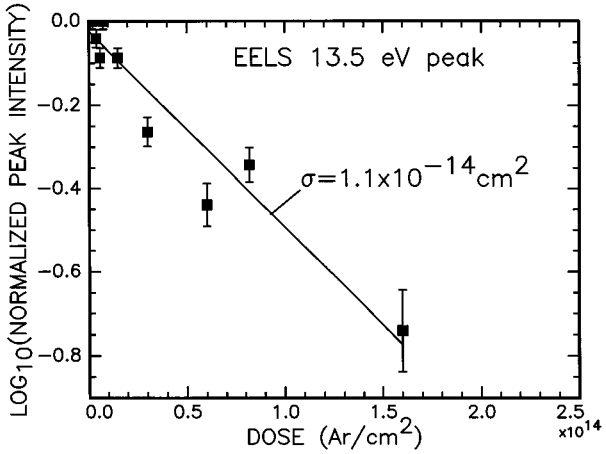

FIG. 6. The diminution of the intensity, I, of the 13.5-eV peak plotted as $\log_{10}(I/I_0)$ vs Ar-ion dose, where I_0 is the intensity of the 13.5-eV peak in the unirradiated film. The straight line is a least-squares linear fit to the data.

show that the data follow the dependence expected from Eq. (1). The straight lines in Figs. 6 and 7 are a least-squares linear fit to the data, which yield cross sections of $(1.1\pm0.1)\times10^{-14}$ and $(0.61\pm0.05)\times10^{-14}$ cm^2 from the diminution of the 13.5- and 17.5-eV peaks, respectively. The cross sections derived from these two peaks are slightly different. This may be partially attributable to the slight broadening, which is observed for the 17.5-eV peak as a function of ion dose, which would tend to result in an underestimate of the cross section. Nevertheless, for the purposes of comparison with the work of others, we take the average of these two values as the determined cross section.

As mentioned above, the ion-beam-induced transformation of C_{60} is driven primarily by nuclear knock-on damage effects. As such, the cross section should scale with the nuclear stopping power $(dE/dx)_{\text{nuclear}}$ rather than $(dE/dx)_{\text{electronic}}$ or $(dE/dx)_{\text{total}}$. Indeed a direct scaling between the dose required to convert half of the C_{60} film to

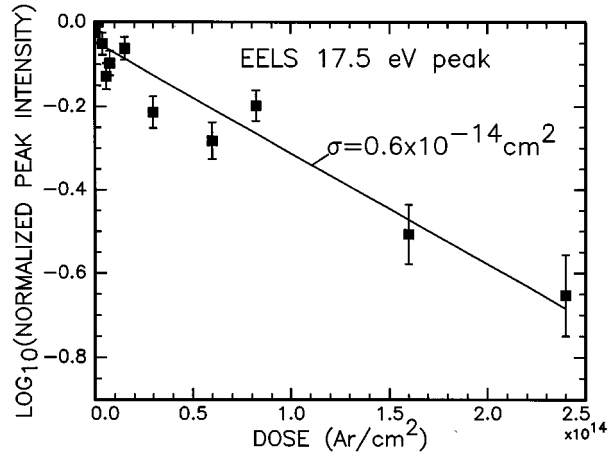

FIG. 7. The diminution of the intensity, I, of the 17.5-eV peak plotted as $\log_{10}(I/I_0)$ vs Ar-ion dose, where I_0 is the intensity of the 17.5-eV peak in the unirradiated film. The straight line is a least-squares linear fit to the data.

TABLE I. The experimentally determined cross section, σ, for various ion species and energies, together with their electronic and nuclear energy losses, as calculated by TRIM (Ref. 11). The cross sections for the 160-keV H, 300-keV He, 300-keV C, and 220-keV Ar implantations have been extracted from the data of Ref. 6, using Eq. (2) (see text).

Ion	Energy (keV)	Experimental cross section (cm^2)	Electronic energy loss (eV/Å/ion)	Nuclear energy loss (eV/Å/ion)
H	100[a]	6.1×10^{-17}	11.7	0.0104
H	160[b]	5.0×10^{-17}	10.8	0.0083
He	300[b]	2.2×10^{-16}	28.7	0.087
C	300[b]	2.05×10^{-15}	47.1	1.9
Ar	220[b]	3.85×10^{-14}	65.3	39.7
Ar	2[c]	0.85×10^{-14}	21.6	49.1
Xe	640[d]	6.0×10^{-13}	223	156

[a]Reference 10.
[b]Reference 6.
[c]The present work.
[d]Reference 5.

amorphous carbon and $(dE/dx)_{\text{nuclear}}$ has been found[6] for implantations with H (160 keV), He (300 keV), C (300 keV), and Ar (220 keV). Assuming that the amorphization of the films follows an exponential dependence similar to that described above for the destruction of C_{60}, the dose for the conversion of 50% of the C_{60} to amorphous carbon $D(I_{a-c}=0.5)$, should be related to the cross section, σ, by the simple relation

$$\sigma = \text{Ln } 2/D(I_{a-c}=0.5). \tag{2}$$

In Table I, we summarize the data for σ extracted from the $D(I_{a-c}=0.5)$ data of Ref. 6, using the above expression, together with the values of σ determined from previous work on 100-keV H,[10] 640-keV Xe,[5] and the 2-keV Ar irradiations of the present work. Note the agreement between the value of σ determined as above for 160-keV H irradiations from Ref. 6 and that determined directly from IR measurements for 100-keV H irradiations (from Ref. 10). This agreement indicates that the procedure of converting from $D(I_{a-c}=0.5)$ to σ is valid. Also included in Table I are the nuclear and electronic energy losses deposited in the film for each ion used, as calculated using the TRIM (Ref. 11) code. The output from TRIM provides files of the ionization loss for both the primary ion and the knock-on C atoms in the collision cascade. The sum of these losses has been used to estimate $(dE/dx)_{\text{electronic}}$ in Table I. TRIM also provides an output file of the total energy imparted to recoils in the collision cascade and this was the data used to estimate $(dE/dx)_{\text{nuclear}}$ in Table I. For all cases, except that of the 2-keV Ar irradiations, the energy loss has been averaged over the first 200 nm of the film thickness as this is a reasonable estimate of the skin depth of the Raman measurements used to determine the cross sections. For the 2-keV Ar irradiations, the skin depth of the *in situ* EELS spectroscopy (based on the elastic mean free path of 1-keV electrons) is estimated to be about 2 nm and hence the energy loss has been averaged over this depth.

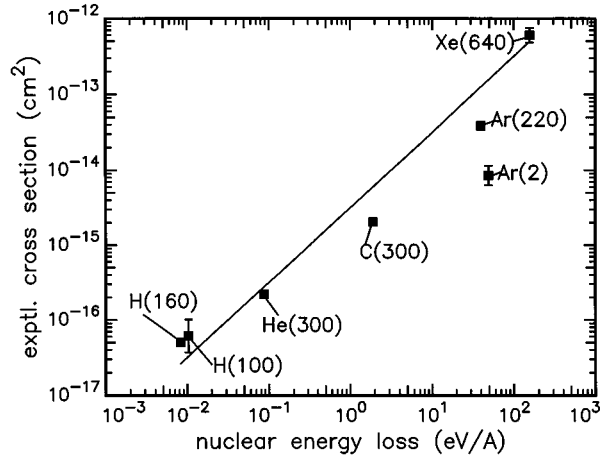

FIG. 8. The experimentally determined cross section, σ, plotted versus the nuclear energy loss per incident ion, as determined by TRIM calculations. The straight line is of unitary slope.

In Fig. 8, σ is plotted as a function of the nuclear energy loss for the results listed in Table I. The straight line is of unitary slope, which should be expected for $\sigma \propto (dE/dx)_{\text{nuclear}}$. The data for all the ions studied follow this dependence reasonably well, except, notably, for the sample irradiated with 2-keV Ar. For this sample, the value of σ is clearly much lower than expected. In particular, note that σ for 2-keV Ar ions is a factor of 4.8 lower than that for 220-keV Ar irradiations, despite the fact that the nuclear energy loss is very similar for these two cases (see Table I and Fig. 8).

As mentioned above, the cross section for irradiation with 640-keV Xe yields an effective radius of 4.6 nm, which is much larger than the geometric radius of the C_{60} molecule. This large effective radius can be explained in terms of the secondary processes, which occur within the collision cascade accompanying the passage of each Xe ion through the solid. Each time a C atom is knocked out of a C_{60} molecule, it has the potential to itself destroy other C_{60} clusters within the 200-nm modified layer. This ''multiplying'' effect explains why the effective radius is so much larger than the geometric radius of a C_{60} cluster. A similar multiplying effect is expected for the other ions used, the magnitude of which decreases with decreasing $(dE/dx)_{\text{nuclear}}$.

Interestingly, for the 2-keV Ar irradiation the effective cross section is about 0.52 nm, which is close to the outer radius of a single C_{60} molecule (0.51 nm).[12] As pointed out above, the value for σ is smaller than that expected, based only on the scaling of the nuclear energy loss. This may indicate that for low energies, the TRIM calculations of nuclear and electronic energy loss are inaccurate, and that a full TRIM simulation of all primary and secondary collision processes (including surface sputtering) may be necessary. At present, it appears that the scaling argument based on nuclear energy deposition alone overestimates the probability that a knocked-on C atom will succeed in destroying another C_{60} molecule. For diamond implanted at low energies, a similar effect is seen in that the critical dose for amorphization of diamond using 40-keV Ar ions is 3.7×10^{14} Ar/cm^2, whereas for 1-keV Ar ions the critical dose is a factor of 5.7 higher, viz., 2.1×10^{15} Ar/cm^2.[13] This factor of about 5.7 compares well to a value of 4.8 for the ratio found in the present work of the cross sections for 220-keV Ar and 2-keV Ar irradiation of C_{60}. Thus, for low-energy irradiation, it appears that the nuclear stopping power is not the only factor which needs to be taken into account.

Although possible, it seems unlikely to be a coincidence that the cross section for destruction of C_{60} using 2-keV Ar ions corresponds almost exactly to the geometric cross section of the C_{60} molecules in the C_{60} film. Hence, it appears that the interaction of each Ar ion with the surface of the film leads to the destruction of one C_{60} molecule. TRIM calculations[14] show that on average, the first interaction of the incoming Ar ion with a C_{60} molecule imparts about 160 eV to the target C atom. The binding energy of the C_{60} molecule is about 400 eV,[12] but the removal of the C atom from the molecule may leave it in an excited and unstable state leading to its disintegration. Some support for this picture may come from recent calculations on the fragmentation of C_{60} clusters.[3] These calculations showed that once the bonds start breaking (which requires temperatures of the order of 4000 K), the fragmentation process occurs very rapidly, within a picosecond.

CONCLUSIONS

The results of this study may be summarized as follows.

(1) With care to the experimental conditions, the EELS spectrum of C_{60} may be measured without degradation during the electron bombardment. The spectrum provides a fingerprint characteristic to the fullerene film.

(2) C_{60} films are gradually amorphized by 2-keV Ar-ion bombardment. No evidence for polymerization or fragmentation into smaller fullerene components was found.

(3) The cross section for the destruction of C_{60} by 2-keV Ar ions was found to be $(0.85\pm0.2)\times10^{-14}$ cm^2. This value gives an effective radius of about 0.52 nm, which is very close to the outer geometric radius of the C_{60} molecule within the fullerene film. Hence, it appears likely that upon impact, on average, each impinging Ar ion destroys one C_{60} molecule.

(4) The cross section for destruction was found to be a factor of about 5 smaller than that expected on the basis of a comparison with the results for bombardment of C_{60} with ions of kinetic energies in the 100–300 keV range. A similar result was found for 2-keV Ar irradiations of diamond in that the critical dose for amorphization was much larger than expected. These examples may indicate that for low-energy ion irradiation, the nuclear stopping power is not the only factor which needs to be taken into account.

ACKNOWLEDGMENTS

S.P. would like to thank the staff of the Solid State Institute of the Technion for their ongoing hospitality, and A.H. would like to acknowledge the financial support of the Department of Applied Physics, Royal Melbourne Institute of Technology.

[1] D. M. Gruen, Nucl. Instrum. Methods Phys. Res. Sect. B **78**, 118 (1993).
[2] A. M. Rao, P. Zhou, K.-A. Wang, G. T. Hager, J. M. Holden, Y. Wang, W. T. Lee, X. X. Bi, P. C. Eklund, D. S. Cornett, M. A. Duncan, and I. J. Amster, Science **259**, 955 (1993).
[3] E. Kim, Y. H. Lee, and J. Y. Lee, Phys. Rev. B **48**, 18 230 (1993).
[4] R. Kalish, A. Somoiloff, A. Hoffman, C. Uzan-Saguy, D. McCulloch, and S. Prawer, Phys. Rev. B **48**, 18 235 (1993).
[5] S. Prawer, K. W. Nugent, S. Biggs, D. McCulloch, W. H. Leong, A. Hoffman, and R. Kalish, Phys. Rev. B **52**, 841 (1995).
[6] J. Kastner, H. Kuzmany, and L. Palmetshofer, Appl. Phys. Lett. **65**, 543 (1994).
[7] P. L. Hansen, P. J. Fallon, and W. Kratschmer, Chem. Phys. Lett. **181**, 367 (1991).
[8] H. Cohen, E. Kolodney, T. Maniv, and M. Folman, Solid State Commun. **81**, 183 (1992).
[9] D. McCulloch, A. Hoffman, and S. Prawer, J. Appl. Phys. **74**, 135 (1993).
[10] R. G. Muscat, R. A. Hawley-Fedder, and W. L. Bell, Radiat. Eff. Defects Solids **118**, 225 (1991).
[11] J. F. Zeigler, J. P. Biersack, and V. Littmark, *The Stopping and Range of Ions in Solids* (Pergamon, New York, 1985).
[12] M. S. Dresselhaus, G. Dresselhaus, and P. C. Eklund, J. Mater. Res. **8**, 2054 (1993).
[13] A. Hoffman, S. Prawer, and R. Kalish, Phys. Rev. B **45**, 12 736 (1992).
[14] T. Shanan (private communication).